



Enhanced Photocatalytic activity of Copper doped and C, N, S codoped TiO₂ Nanoparticles on Methylene Blue dye under Solar light irradiation

A Nixon Thangaraj^{1*}, C. Ravi Samuel Raj² and W. Jose Benita Regilet³

¹Department of Chemistry, VV College of Engineering, Tisayanvilai - 628 656, Tamilnadu, India

²Department of Chemistry, Pope's College, Sawyerpuram - 628 251, Tamilnadu, India.

³M. Phil Scholar, Department of Chemistry, Pope's College, Sawyerpuram - 628 251, Tamilnadu, India.

Abstract : TiO₂ nanoparticles (TNPs) doped with copper (Cu) and codoped with carbon (C), nitrogen (N) and sulfur (S) was prepared and characterized using diffuse reflectance UV-Vis spectroscopy, FT-IR, XRD and EDX. Photocatalytic degradation behaviour of these photocatalysts was investigated by studying degradation of Methylene Blue (MB) dye in aquatic medium under solar light irradiation. The effect of various operational parameters for photodegradation such as initial concentration of MB dye, dose of photocatalyst and irradiation time was investigated in order to attain highest photocatalytic degradation efficiency. The photocatalytic degradation reaction kinetics of MB dye using the prepared photocatalysts was also studied. An appropriate mechanism has been proposed and the effect of doping on photocatalytic degradation behaviour of the above photocatalysts also discussed.

Introduction

The availability of potable water in nature is becoming very rare day by day¹. Water around the world is getting polluted mainly by both human activities and industrial effluents. Textile industries play a vital role in the economy and employment of many countries. Same time, 20% of world's water pollution is caused by textile industries. These textile industries use more than 8000 chemicals and dyes in a year all around the world. Textile dyes are one of the major contaminants in effluent from textile industries around the world².

Methylene blue (MB) is basic aniline dye, one among the powerful organic dyes generally used in textile, dyeing, pesticide, printing, temporary hair colouring industries and coating for paper stock³. MB dye is also used in many industries such as pulp mill, leather and plastic⁴. MB dye causes eye burns, which may be responsible for permanent injury to the eyes of human and animals. On inhalation, it can give rise to short periods of rapid or difficult breathing, while ingestion through the mouth produces a burning sensation and may cause nausea, vomiting, profuse sweating, mental confusion, painful micturition, and methemoglobinemia⁵. Because of its aromatic ring, MB is highly toxic and very difficult to degrade. The existence of MB dye in water, even the concentration is low, is highly noticeable and disagreeable. Hence this dye has to be removed from water source before discharging into environment⁶.

Recently, there has been considerable interest on the ability of the photocatalytic technique to completely degrade organic dyes into water and CO₂, without generating any harmful by-products⁷. Using

direct photocatalytic reaction by semiconductor powder like TiO_2 as photocatalysts has been shown to effectively degrade many kinds of pollutants including dye pollutants and in many cases even completely mineralize the compounds⁸.

TiO_2 has been extensively studied as a photocatalyst due to its non toxicity, thermal stability, chemical stability, high photocatalytic activity and low cost. In the recent years TiO_2 nanoparticles (TNPs) is considered to be the most suitable photocatalyst for the degradation of organic dyes and other pollutants⁹. These TNPs can be easily synthesized by sol-gel route. In general, it was reported that the doping of TNPs with transition metal cations is a good method to enhance photocatalytic properties and for the enhancement of visible light response¹⁰. The addition of transition metal cations cause the development of doping energy level between valence band and conduction band of TiO_2 and translocation the band gap of TiO_2 into the visible region. Further, metal dopant cations can act as a trap for electrons or holes and enhances the photocatalytic activity of TiO_2 under the visible light¹¹. In photocatalysis, doping with metal and non-metal also has been extensively investigated¹².

In this work, we synthesized and characterized undoped TNPs, copper doped (Cu-TNPs) and copper and thiourea codoped TNPs (Cu-TU-TNPs). Also, the potential of TNPs as a photocatalyst under solar light radiation for the removal of MB dyewas investigated. The effect of three important operational parameters such as effect of initial concentration, effect of dose of the catalyst and effect of irradiation time was explored.

Experimental

Materials and methods

Titanium isopropoxide from Sigma Aldrich, Copper chloride dihydrate, Thiourea and absolute ethanol from Merck, Nitric acid, RhB dye from Himedia were purchased. Ultraviolet-visible spectroscopy (UV-Vis) was analyzed using a JASCO V-670 UV-VIS Spectrophotometer. Formation of TiO_2 nanoparticles was checked using Fourier transform infrared spectroscopy (FTIR) in Perkin-Elmer Spectrum-1 instrument with freshly dried KBr pellets in the range of $4000\text{-}400\text{ cm}^{-1}$. Powder X-ray diffraction (XRD) measurements were recorded with D8 advance Bruker AXS diffractometer using $\text{CuK}\alpha$ radiation ($\lambda = 1.5406\text{ \AA}$). Alumina was used as a standard to eliminate instrument peak broadening. EDX analysis was used for the elemental analysis and determination of chemical compositions of the sample. EDX were examined by FE-SEM (JSM-6700F, JEOL, Japan) equipped with an in-situ EDX spectrophotometer. The photocatalytic degradation of MG dye was studied in the presence of solar light irradiation. 100 ml borosilicate glass beakers were utilised as reaction vessel throughout the photocatalytic degradation experiment.

In each experiment, photocatalysts were suspended in 30 mL of MB dye solution with various concentrations taken in a reaction vessel. This reaction vessel was constantly stirred for the photodegradation treatment under solar light irradiation for 2 hours. A small portion of the mixture was withdrawn before and after irradiation (every half an hour for effect of irradiation time). The mixture was centrifuged immediately and the supernatant was evaluated as the measurement of the residual dye concentration. The absorption maxima were measured by using UV-vis spectrophotometer.

Synthesis of photocatalysts

In recent years, synthesis of photocatalysts such as undoped TNPs, Cu-TNPs and Cu-TU-TNPs has been well-known and their synthetic methods were presented noticeably in many literatures¹³. Initially, 8.4 mL titanium (IV) isopropoxide (TiP) was dissolved in 10 mL absolute ethanol (Solution A). Another solution named as Solution B consists of 10 mL absolute ethanol, 1 mL concentrated HNO_3 and 1 mL of distilled water, was added drop wise to solution A, and then, the mixture was constantly stirred for 18 hours to form a wet-gel. Further, the wet-gel was left aside for 6 hours and then dried at $110\text{ }^\circ\text{C}$ for 15 hours in hot air oven. Finally, TiO_2 nanopowder was calcined at $300\text{ }^\circ\text{C}$ for 5 hours.

In order to synthesize Cu-TNPs and Cu-TU-TNPs, same synthetic procedure was followed by adding 0.097 grams of $\text{CuCl}_2 \cdot 2\text{H}_2\text{O}$ (which is equal to 1% of TiO_2 mass) and 0.0432 grams of Thiourea (which is equal to 1% of TiO_2 mass) to solution B respectively along with the TiO_2 precursor.

Results and Discussion

Absorption Spectra

Figure 1 shows that the Ultra violet-visible diffuse reflectance (UV-Vis DRS) spectra of undoped TNPs, Cu-TNPs and Cu-TU-TNPs. Band gap was calculated using Kubelka-Munk formulae for all the synthesized photocatalysts¹⁴ from the spectra. Band gap is one among the significant characters which help to understand the photocatalytic activity of the prepared samples¹⁵. The band gap is found to be 2.91, 2.89 and 2.85 for undoped TNPs, Cu-TNPs and Cu-TU TNPs respectively. Band gap of TNPs, prepared by the same synthetic procedure was reported to be 2.85 nm. From the values of band gap, it has been evidently revealed that the doping of copper and thiourea have brought minor changes on their band gap value when compared with undoped TNPs. The decrement in the band gap value after doping improves the photocatalytic behaviour of the photocatalyst¹⁶.

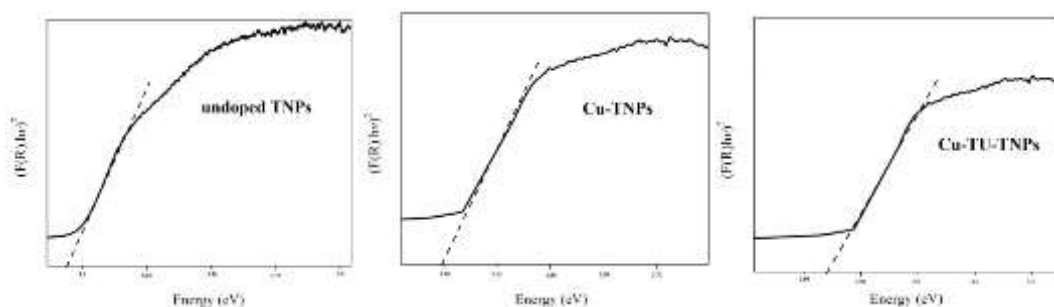


Figure 1 UV-Vis DRS of undoped and doped TNPs (Kubelka-Munk model)

FT-IR spectra

The FT-IR spectra of undoped TNPs, Cu-TNPs and Cu-TU-TNPs are depicted in Figure 2. The FT-IR spectra of all the samples show peaks near at 3200 cm^{-1} and 1620 cm^{-1} . These two peaks showed the presence of traces of moisture in all the samples. In the FT-IR spectra of undoped TNPs, a broad band at 3248 cm^{-1} and a band at 1620 cm^{-1} were aroused due to moisture. Importantly, the band at 478 cm^{-1} was ascribed to the Ti-O bending mode of TiO_2 which confirmed the formation of TNPs¹⁷. Moreover, the peak was shifted after doping. In the case of Cu-TNPs, the later peak was shifted to 448 cm^{-1} , which might be due to the formation of Cu-O bond¹⁸. In the FT-IR spectra of Cu-TU-TNPs, the peak observed at 1092 cm^{-1} showed the presence of C=S bond¹⁹. The other peak related to thiourea was not observed. This might be due to the lower percentage of doping.

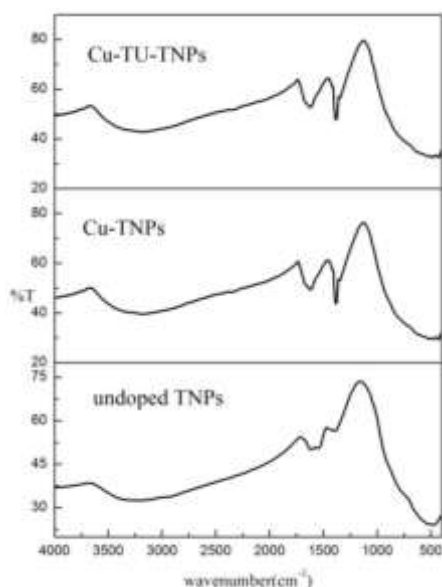


Figure 2 FT-IR spectra for doped and undoped TNPs

XRD Analysis

Figure 3 shows that the XRD studies of TiO₂ nanoparticles and the results were well agreed with the previous studies. In the X-ray diffraction pattern of undoped TNPs, a main peak (2θ) at 25.4° attributed to the 1 0 1 planes (JCPDS 21-1272) of anatase phase. There is no observation of peak at 2θ near at 27° indicates the absence of any rutile phase in the synthesised TNPs²⁰. 25.3°(2θ) and 25.4°(2θ) are the major peaks observed for Cu-TNPs and Cu-TU-TNPs respectively. These values clearly indicate that doping of copper did not cause any deviation in the major peaks²¹. The reason for this might be due to the occupation of guest metal ions in the substitutional sites of titanium ions in the host lattice of TNPs. Further in the XRD patterns of Cu-TU-TNPs, thiourea was not observed. This might be due to the lower percentage of doping.

The average interplanar distance (d) and the average crystallite size were calculated using Debye-Scherrer equation. The average interplanar distance was found to be 3.53Å, 3.45 Å and 3.52 Å for undoped TNPs, Cu-TNPs and Cu-TU-TNPs respectively. The average crystallite size was found to be 3.87nm, 3.15 nm and 4.41 nm for undoped TNPs, Cu-TNPs and Cu-TU-TNPs respectively.

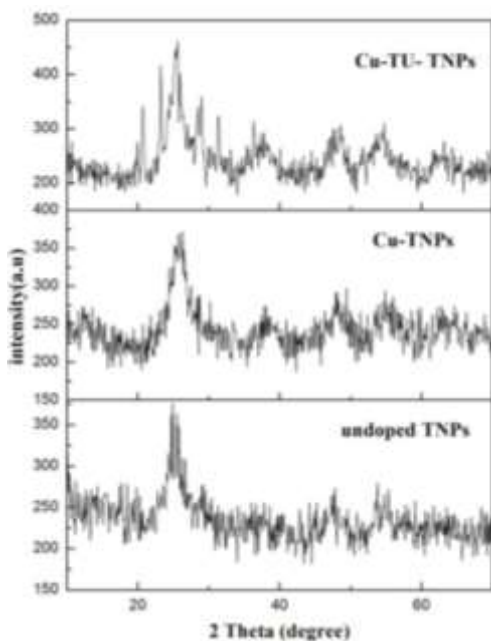


Figure 3 XRD pattern of doped and undoped TNPs

EDX Analysis

Figure 4 and 5 represents the EDX analysis for undoped TNPs and Cu-TNPs, which were used for the elemental analysis and determination of chemicals present in the TNPs. The result clearly shows that the doping of copper in TNPs was proceeded well. Further, the compositional analysis of synthesized Cu-TNPs, the weight percentage ratio of Copper in Cu-TNPs was found to be 1.09.

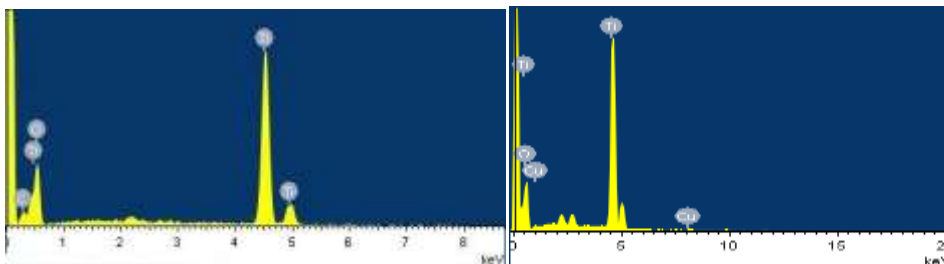


Figure 4 EDX behavior of undoped TNPs Figure 5 EDX behavior of Cu- TNPs

Effect of initial concentration

Photocatalytic degradation of MB dye was studied at different initial concentrations ranging from 15 to 75 ppm in the presence of undoped TNPs, Cu-TNPs and Cu-TU-TNPs under solar light irradiation.

From this experiment it is noted that the dye degradation rate was decreased with increase in the initial concentration of dyes. Whenever the concentration of dye solution increases, the photons get interrupted before they can reach the surface of the catalyst and thus decreases the absorption of photons by the photocatalysts. Due to this reason, the photocatalytic degradation rate of the dyes with higher concentration gets reduced²² and more dye molecules are adsorbed on the surface of the photocatalysts by increasing the concentration of dyes which results the occupation of active sites of the photocatalysts²³. Hence, the photocatalytic degradation rate of MB dye was decreased with increase of concentration of dyes. The optimum concentration of MB dye is fixed as 45 ppm for further studies.

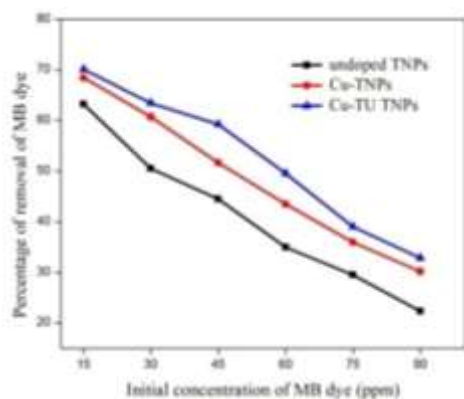


Figure 6 Effect of initial concentration of MB dye under solar light irradiation

Table 1 Effect of initial concentration of MB dye under solar light irradiation

Initial concentration of MB dye (in ppm)	Percentage removal of MB dye (%)			Reaction medium conditions
	undoped TNPs	Cu-TNPs	Cu-TU-TNPs	
15	63.2	68.46	70.1	Irradiation time = 120 minutes
30	50.49	60.72	63.43	
45	44.5	51.66	59.22	
60	34.94	43.49	49.51	Catalyst concentration = 30 mg
75	29.51	35.96	39.04	
90	22.33	30.17	32.87	

From the results, it was observed that the photocatalytic degradation efficiency of photocatalyst was improved with an increase amount of photocatalysts up to 1.333 g/L, and after that there is no significant change in the rate of photocatalytic degradation. The decrease in availability of vital active sites and the penetration of solar light into the suspension formed causes decrement rate of photocatalytic activity of photocatalysts²⁴. The suspension of higher amount of photocatalyst (>1.33 g/L) to the MB dye solution increases the turbidity in the suspension and subsequently there is a decrease of solar light penetration due to increased scattering effect. In addition, at high photocatalyst loading, it is very hard to retain the suspension as homogenous due to particles agglomeration, which decreases the number of vital active sites²⁵. Thus, the most effective photocatalytic degradation was observed at 1.33 g/L of all photocatalysts and the amount was fixed as optimum dose for further experiments.

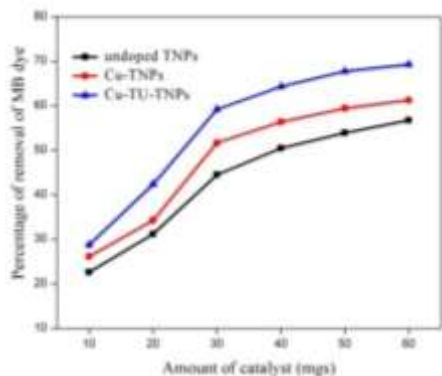


Figure 7 Effect of dose of the photocatalyst on MB dye under solar light irradiation

Table 2 Effect of dose of the photocatalyst on MB dye under solar light irradiation

Dose of the catalysts (in mg)	Percentage removal of MB dye (%)			Reaction medium conditions
	undoped TNPs	Cu-TNPs	Cu-TU-TNPs	
10	22.61	26.14	28.71	Catalyst concentration = 30 mg
20	31.17	34.28	42.37	
30	44.5	51.66	59.22	
40	50.46	56.39	64.33	MB dye concentration = 45 ppm
50	53.89	59.45	67.77	
60	56.75	61.27	69.28	

Effect of irradiation time

Irradiation time plays an essential role in the photocatalytic degradation process of the MB dye. The irradiation time is differed from 30 minutes to 180 minutes for MB dye in presence of undoped TNPs, Cu-TNPs and Cu-TU-TNPs under solar light irradiation.

From the experiment it was observed that the dye degradation rate increased with increase of irradiation time²⁶. This might be due to low light intensity reactions where electron-hole formation is pivotal and electron-hole recombination is insignificant and considerably negligible²⁷. Although, when light intensity increases the electron-hole pair separation emulates with recombination and causes lower effect on the rate of the reaction²⁸. The optimum time for MB dye is fixed as 120 min for further studies.

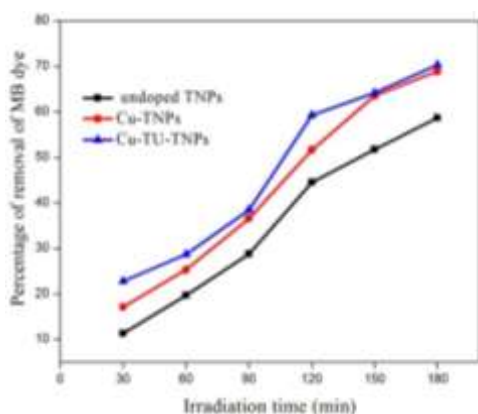


Figure 8 Effect of irradiation time on MB dye under solar light irradiation

Table 3Effect of irradiation time on MB dye under solar light irradiation

Irradiation time (in min)	Percentage removal of MB dye (%)			Reaction medium conditions
	undoped TNPs	Cu-TNPs	Cu-TU-TNPs	
30	11.35	17.15	22.81	Irradiation time = 120 minutes
60	19.68	25.31	28.67	
90	28.74	36.59	38.43	
120	44.5	51.66	59.22	MB dye concentration = 45 ppm
150	51.71	63.55	64.17	
180	58.66	68.89	70.28	

Pseudo First order kinetics

The photocatalytic degradation processes of MB dye is inclined to string along with pseudo-first-order kinetics in presence of the undoped TNPs, Cu-TNPs and Cu-TU-TNPs under solar light irradiation. The linearity of plot suggests that the photo decolouration reaction approximately follows the pseudo-first order²⁹.

Table 4Pseudo-first order kinetics for MB dye degradation under solar light irradiation

Irradiation time (in min)	$\ln C_0/C_t$			Reaction medium conditions
	undoped TNPs	Cu-TNPs	Cu-TU-TNPs	
30	0.1205	0.1881	0.2589	Irradiation time = 120 minutes
60	0.2192	0.2918	0.3379	
90	0.3388	0.4555	0.4850	
120	0.5888	0.7269	0.8970	MB dye concentration = 45 ppm
150	0.7279	1.0092	1.0264	
180	0.8833	1.1676	1.2133	

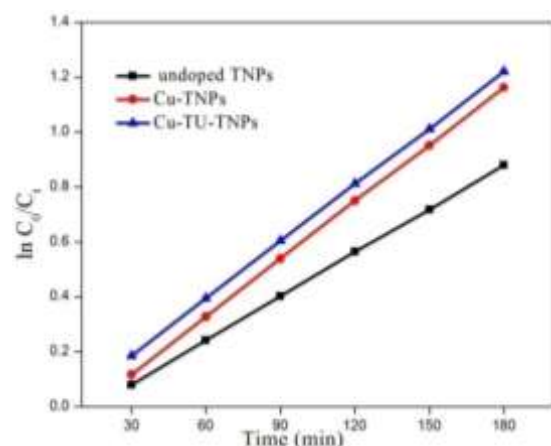
**Figure 10** Determination of pseudo-first order kinetic rate constant for MB dye degradation under solar light irradiation

Table 4 and Figure 9 showed the kinetics of degradation of MB dye for an initial concentration of 45 mg/L under optimized conditions. The regression curve of natural logarithm of MB dye concentration *versus* irradiation time gives straight line in all the cases (i.e. undoped TNPs, Cu-TNPs and Cu-TU-TNPs). The experimental results for MB dye give a straight line and fit well with pseudo-first order kinetics. This result shows that the photocatalytic degradation of MB dye occurs only on the surface of the photocatalysts and follows pseudo-first order kinetics³⁰.

Langmuir-Hinshelwood kinetics

Langmuir-Hinshelwood (L-H) kinetics model is used to describe the behaviour of photocatalytic degradation of many organic dyes³¹. The L-H model can be written as follows

$$\frac{1}{r} = \frac{1}{kKC} + \frac{1}{k} = \frac{1}{k_{obs}}$$

Table 5 showed the values of $\ln C_0/C_t$ for all the synthesized photocatalysts. Figure 11a, 11b and 11c showed the plot of $\ln C_0/C_t$ vs irradiation time in minutes. From the plot, the slope, intercept and R^2 values have been calculated using linear regression method. Figure 12 shows our results that a straight line according to L-H model, through a plot of $1/k_{obs}$ vs initial concentration forms.

Table 5 $\ln C_0/C_t$ values for MB dye degradation in the presence of catalysts under solar light irradiation

Irradiation time (in min)	$\ln C_0/C_t$ (15 ppm)			$\ln C_0/C_t$ (30 ppm)			$\ln C_0/C_t$ (60 ppm)		
	undoped TNPs	CuTNPs	Cu-TU-TNPs	undoped TNPs	Cu-TNPs	Cu-TU-TNPs	undoped TNPs	Cu-TNPs	Cu-TU-TNPs
30	2.5321	2.6056	2.6985	2.4712	2.5463	2.6268	0.0447	0.0932	0.194
60	2.6428	2.7227	2.7896	2.575	2.6563	2.7113	0.1359	0.1871	0.2678
90	2.779	2.911	2.9625	2.7017	2.8314	2.8701	0.2454	0.3332	0.4043
120	3.0717	3.2353	3.477	2.9694	3.1267	3.327	0.4704	0.5694	0.7775
150	3.2408	3.5951	3.6516	3.1208	3.443	3.4754	0.593	0.8052	0.8915
180	3.4363	3.8113	3.9201	3.2922	3.6257	3.6953	0.7274	0.9324	1.0529

The rate constants are calculated to be $61.47 \times 10^{-5} \text{ Mmin}^{-1}$, $42.91 \times 10^{-5} \text{ Mmin}^{-1}$ and $42.82 \times 10^{-5} \text{ Mmin}^{-1}$ for undoped TNPs, Cu-TNPs and Cu-TU-TNPs respectively. Similarly the adsorption equilibrium constants are calculated to be $1.6746 \times 10^{-5} \text{ M}^{-1}$, $1.6493 \times 10^{-5} \text{ M}^{-1}$ and $1.5687 \times 10^{-5} \text{ M}^{-1}$ for undoped TNPs, Cu-TNPs and Cu-TU-TNPs respectively.

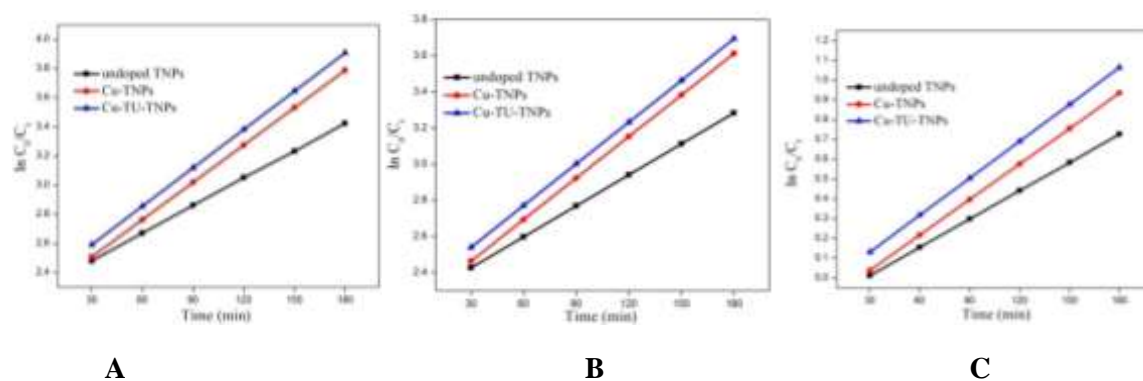


Figure 11 $\ln C_0/C_t$ vs Time (min) for MB dye degradation in the presence of catalysts under solar light irradiation A) 15 ppm B) 30 ppm C) 60 ppm

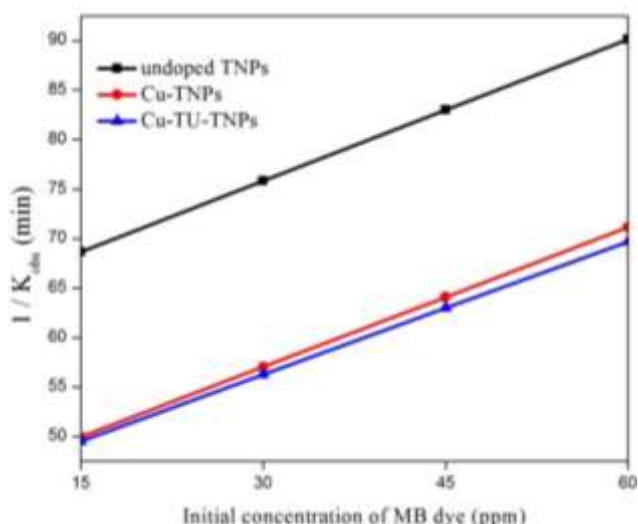
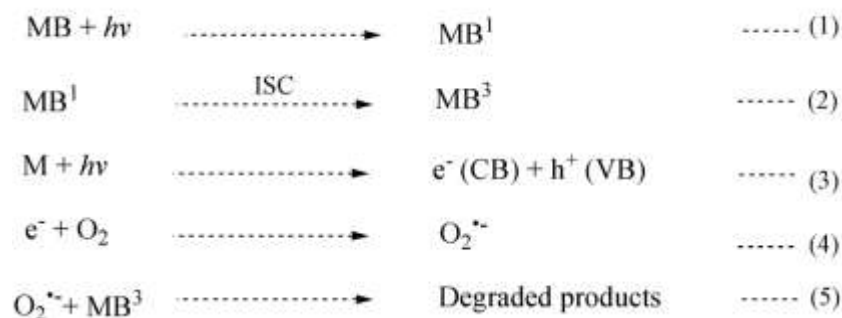


Figure 12 Determination of the adsorption equilibrium constant and the reaction rate constant of MB dye degradation in the presence of catalysts under solar light irradiation for the Langmuir-Hinshelwood kinetic model

These experimental results of MB dye fit well with L-H model kinetics. These results show that the photocatalytic degradation of MB dye occurs on the surface of the photocatalysts and follows L-H model kinetics^{32,33}.

Mechanism of photocatalytic degradation of MB dye

On the basis of the previous studies^{34,35}, a speculative mechanism for photocatalytic degradation of MB dye may be proposed as follows.



Under solar light irradiation, MB dye molecule absorbs radiation and jumps first to singlet state (6) and then through inter system crossing (ISC) to triplet state (7) which transfers an electron from its HOMO to the conduction band. Meanwhile, the synthesised TNPs and metal doped TNPs (M) absorb the incident light energy which excites the electron from HOMO level to conduction band (8). The electrons present at the conduction band of both dye and TNPs and the surface adsorbed oxygen are responsible for the photocatalytic degradation of MB dye (9, 10) and results harmless degraded product.

Conclusion

Undoped TNPs, Cu-TNPs and Cu-TU-TNPs were synthesized successfully by sol-gel method and UV-vis, FT-IR, XRD and EDX studies established the formation of the above photocatalysts. The photocatalytic degradation behaviour of these photocatalysts was analysed. From the studies, the efficiency of photocatalyst was found to decrease with increase of MB dye concentration, at the same time, increase with increase in dose of photocatalyst and increase with solar light intensity. Further, it was found that the doping with copper and thiourea (C, N, S doping) influence the photocatalytic degradation efficiency of the above photocatalyst. The

kinetic study reports confirm that the photocatalytic degradation of MB dye occurs only on the surface of the undoped TNPs, Cu-TNPs and Cu-TU-TNPs. Further, enhancement of photodegradation of TNPs was also discussed. From the results, doping of TNPs with Cu, C, N and S is the main reason for enhancing the degradation of MB dye.

References

1. Loubet P, Roux P, Loiseau E, Maurel VB. Life cycle assessments of urban water systems: A comparative analysis of selected peer-reviewed literature. *Water Res.*, 2014, 67; 187-202.
2. Ajmal A, Majeed I, Malik RN, Iqbal M, Nadeem MA, Hussain I, Zeshan SY, Mustafa G, Zafar MI, Nadeem MA. Photocatalytic degradation of textile dyes on Cu₂O-CuO/TiO₂ anatase powders. *J. Environ. Chem. Eng.*, 2016, 4(2); 2138-2146.
3. Chena L, Lia Y, Du Q, Wang Z, Xia Y, Yedinak E, Lou J, Ci L. High performance agar/graphene oxide composite aerogel for methylene blue removal. *Carbohydr. Polym.*, 2017, 155; 345-353.
4. Kumar A, Jena HM. Removal of methylene blue and phenol onto prepared activated carbon from Fox nutshell by chemical activation in batch and fixed-bed column. *J. Clean. Prod.*, 2016, 137; 1246-1259.
5. Hameed BH, Din ATM, Ahmad AL. Adsorption of methylene blue onto bamboo-based activated carbon: Kinetics and equilibrium studies. *J. Hazard. Mater.*, 2007, 141; 819-825.
6. Wu Y, Zhang L, Gao C, Ma J, Ma X, Han R. Adsorption of Copper Ions and Methylene Blue in a Single and Binary System on Wheat Straw. *J. Chem. Eng. Data.*, 2009, 54; 3229-3234.
7. Al-Gubury HY and Al-Murshidy GS. Photocatalytic Decolorization of Brilliant Cresyl Blue using Zinc Oxide. *Int. J. PharmTech Res.*, 2015, 8(2); 289-297.
8. Wang J, Xie Y, Zhang Z, Li J, Chen X, Zhang L, Xu R, Zhang X. Photocatalytic degradation of organic dyes with Er³⁺:YAlO₃/ZnO composite under solar light. *Sol. Energy Mater. Sol. Cells.*, 2009, 93; 355-361.
9. Salama TM, Ali IO, Mohamed MM. Synthesis and characterization of mordenites encapsulated titania nanoparticles: Photocatalytic degradation of meta-chlorophenol. *J. Mol. Catal. A: Chem.*, 2007, 273; 198-210.
10. Crisan M, Raileanu M, Dragan N, Crisan D, Ianculescu A, Nitoi I, Oancea P, Somacescu S, Stanica N, Vasile B, Stan C. Sol-gel iron doped TiO₂ nanopowders with photocatalytic activity. *Appl. Catal., A.*, 2015, 504; 130-142.
11. Mesagri Z, Gharagozlou M, Khosravi A, Gharanjig K. Synthesis, characterization and evaluation of efficiency of new hybrid Pc/Fe-TiO₂ nanocomposite as photocatalyst for decolorization of methyl orange using visible light irradiation. *Appl. Catal. A.*, 2012, 411-412; 139-145.
12. Yu S, Yun HJ, Lee DM, Yi J. Preparation and characterization of Fe-doped TiO₂ nanoparticles as a support for a high performance CO oxidation catalyst. *J. Mater. Chem.*, 2012, 22; 12629-12635.
13. Altin I, Sokmen M, Biyiklioglu Z. Quaternized zinc(II) phthalocyanine-sensitized TiO₂: surfactant-modified sol-gel synthesis, characterization and photocatalytic applications. *Desalin. Water Treat.*, 2016, 57; 16196-16207.
14. Lopez R, Gomez R. Band-gap energy estimation from diffuse reflectance measurements on sol-gel and commercial TiO₂: a comparative study. *J Sol-Gel Sci Tech.*, 2012, 61; 1-7.
15. Pan C, Zhu Y. New Type of BiPO₄ Oxy-Acid Salt Photocatalyst with High Photocatalytic Activity on Degradation of Dye. *Environ. Sci. Technol.*, 2010, 44; 5570-5574.
16. Khan MM, Ansari SA, Pradhan D, Ansari MO, Han DH, Lee J, Cho MH. Band gap engineered TiO₂ nanoparticles for visible light induced photoelectrochemical and photocatalytic studies. *J. Mater. Chem. A.*, 2014, 2; 637-644.
17. Bezrodna T, Puchkovska G, Shymanovska V, Baran J, Ratajczak H. IR-analysis of H-bonded H₂O on the pure TiO₂ surface. *J. of Mol. Struct.*, 2004, 700; 175-181.
18. Mugundan S, Rajamannan B, Viruthagiri G, Shanmugam N, Gopi R, Praveen P. Synthesis and characterization of undoped and cobalt-doped TiO₂ nanoparticles via sol-gel technique. *Appl. Nanosci.*, 2015, 5; 449-456.
19. Aitken GB, Duncan JL, McQuillan GP. Normal Co-ordinates for the Planar Vibrations of Thiourea, and Frequency Assignment for Selenourea. *Inorg. Phys. Theor.*, 1971, 2695-2698.

20. Baiju KV, Shajesh P, WunderlichW, MukundanP, Kumar SR, Warriar KGK. Effect of tantalum addition on anatase phase stability and photoactivity of aqueous sol-gel derived mesoporous titania. *J. Mol. Catal. A: Chem.*, 2007, 276; 41-46.
21. HamadaniM, Reisi-Vanani A, Majedi A. Sol-Gel Preparation and Characterization of Co/TiO₂ Nanoparticles: Application to the Degradation of Methyl Orange. *J. Iran. Chem. Soc.*, 2010, 7; S52-58.
22. Chakrabarti S, DuttaBK. Photocatalytic degradation of model textile dyes in wastewater using ZnO as semiconductor catalyst. *J. Hazard. Mater.*, 2004, B112; 269-278.
23. WangW, Silva CG, FariaJL. Photocatalytic degradation of Chromotrope 2R using nanocrystalline TiO₂/activated-carbon composite catalysts. *Appl. Catal., A*, 2007, 70; 470-478.
24. BehnajadyMA, ModirshahlaN, HamzaviR. Kinetic study on photocatalytic degradation of C.I. Acid Yellow 23 by ZnO photocatalyst. *J. Hazard. Mater.*, 2006, B133; 226-232.
25. Rabindranathan S, DevipriyaS, YesodharanS. Photocatalytic degradation of phosphamidon on semiconductor oxides. *J. Hazard. Mater.*, 2003, B102; 217-229.
26. NeppolianB, ChoiHC, SakthivelS, ArabindooB, MurugesanV. Solar light induced and TiO₂ assisted degradation of textile dye reactive blue 4. *Chemosphere*, 2002, 46; 1173-1181.
27. SoCM, ChengMY, YuJC, WongPK. Degradation of azo dye Procion Red MX-5B by photocatalytic oxidation. *Chemosphere*, 2002, 46; 905-912.
28. SauerT, NetoCG, JoseHJ, MoreiraRFPM. Kinetics of photocatalytic degradation of reactive dyes in a TiO₂ slurry reactor. *J. Photochem. Photobiol., A*, 2002, 149; 147-154.
29. ChunH, YizhongW, HongxiaoT. Preparation and characterization of surface bond-conjugated TiO₂/SiO₂ and photocatalysis for azo dyes. *Appl. Catal., B*, 2001, 30; 277-285.
30. Vasanth KumarK. Linear and non-linear regression analysis for the sorption kinetics of methylene blue onto activated carbon. *J. Hazard. Mater.*, 2006, 137(3); 1538-1544.
31. WuJ, HungC, YuanC. Kinetic modeling of promotion and inhibition of temperature on photocatalytic degradation of benzene vapour. *J. Photochem. Photobiol., A*, 2005, 170; 299-306.
32. EmelineAV, RyabchukVK, SerponeN. Dogmas and Misconceptions in Heterogeneous Photocatalysis. Some Enlightened Reflections. *J. Phys. Chem. B.*, 2005, 109; 18515-18521.
33. HerediaJB, TorregrosaJ, DominguezJR, PeresJA. Oxidation of p-hydroxybenzoic acid by UV radiation and by TiO₂/UV radiation: comparison and modelling of reaction kinetic. *J. Hazard. Mater.*, 2001, B83; 255-264.
34. UnalU, MatsumotoY, TamotoN, KoinumaM, MachidaM, IzawaK. Visible light photoelectrochemical activity of K₄Nb₆O₁₇ intercalated with photoactive complexes by electrostatic self-assembly deposition. *J. Solid State Chem.*, 2006, 179; 33-40.
35. ZhaoX, LiZ, ChenY, ShiL, ZhuY. Enhancement of photocatalytic degradation of polyethylene plastic with CuPc modified TiO₂ photocatalyst under solar light irradiation. *Appl. Surf. Sci.*, 2008, 254; 1825-1829.
